Journal of Electronic Testing (2024) 40:657–667
https://doi.org/10.1007/s10836-024-06145-3

RESEARCH

PCB Defect Recognition by Image Analysis using Deep Convolutional Neural Network

Jiantao Zhang[1] · **Xinyu Shi**[1] · **Dong Qu**[1] · **Haida Xu**[1] · **Zhengfang Chang**[1]

Received: 17 July 2024 / Accepted: 3 October 2024 / Published online: 18 October 2024

Abstract
Printed circuit board (PCB) is one of the most important components of electronic products. The traditional defect detection methods are very difficult to meet the defect detection requirements in the PCB production process. In recent years, the Convolutional Neural Networks (CNNs) have developed rapidly and have shown greater advantages than traditional methods in the field of machine vision. In order to reduce the workload of manual inspection and improve production efficiency, the PCB defect image recognition method based on the convolutional neural network is studied in this paper. Three convolutional neural network classification models VGG16, InceptionV3 and ResNet50 are studied. The test results based on the PCB image data set show that the ResNet50 model has better PCB defect image classification capabilities than the VGG16 and InceptionV3 models. It also shows that the classification accuracy of the ResNet50 model can be improved by data augmentation methods, even without increasing the number of PCB image samples. Based on the analysis of the ResNet50 network structure, an improved network model structure is developed. In the ResNet50 model, a new CNN module Res2Net is introduced, which replaces the residual block of the original convolutional layer with a more layered residual connection structure. The Rectified Linear Unit (ReLU) function is used as the activation function behind each BottleNeck to improve the non-linear expansion capability of the network. The experimental results under the same conditions show that the improved ResNet50 model has better classification performance in PCB defect classification tasks.

Keywords PCB Defective Images · Deep Convolutional Neural Network · Deep Learning · Feature Extraction

1 Introduction

With the rapid development of microelectronics technology and computer technology, the microelectronics industry has developed rapidly [1]. The PCB industry become the foundation of the entire electronics industry chain. As the continuous improvement of PCB production level, the requirements for PCB performance are getting higher and higher. However, due to the complexity of the PCB manufacturing process, the quality of the PCB products produced is uneven. Therefore, PCB defect detection is particularly important in the entire PCB product production process [2]. PCB defects can be categorized into two main types: external observable features and internal observable features. The external observable features can be further subdivided into several subclasses including printed circuit board edges, solder mask layers, substrate surfaces, and plated holes. Defects in these external features, such as discoloration of the gold surface, burrs, skip plating, residues, foreign objects, and scratches, can usually be identified using visual inspection techniques. Internal observable features include conductive patterns and dielectric materials. Detecting these features often requires more complex techniques, such as electrical testing or cross-sectional analysis of conductors [3]. The commonly used methods of PCB defect detection mainly include manual detection methods, machine vision-based detection methods, and deep learning-based detection methods [4]. Traditional PCB defect detection is usually based on manual visual inspection. The inspectors find PCB defects by visual comparison and observation with the help of optical aids such as magnifying glasses [5]. This method has a good detection effect for small batches and low-complexity

Responsible Editor: V. D. Agrawal

✉ Jiantao Zhang
zhangjt@shu.edu.cn

[1] School of Mechatronic Engineering and Automation Shanghai Key Laboratory of Intelligent Manufacturing and Robotics, Shanghai University, Shanghai, China

microchips. Once the number or complexity of PCBs increases, inspectors are prone to visual fatigue, which can easily lead to errors and omissions. The inspection efficiency and accuracy will also be reduced.

In order to overcome disadvantages of traditional PCB defect detection methods, automatic optical inspection (AOI) systems have gradually been used in PCB defect detection [6–8]. AOI uses machine vision technology and image processing methods to detect PCB defects. This method improves production efficiency and detection quality stability. Currently, the final inspection of many PCB products adopts the AOI method [9–11].

In recent years, deep learning has developed rapidly, and convolutional neural networks have made breakthroughs in the fields of machine vision, image classification, target detection, and intelligent robots [12–14]. Convolutional neural networks are particularly well-suited for image processing. CNNs mimic the workings of the human visual system, effectively recognizing and categorizing objects within images. This network architecture excels in processing data with hierarchical structures, such as images, because it can capture features at multiple levels. A typical CNN includes several convolutional layers, activation layers, and pooling layers. These layers learn local features within images, gradually building a comprehensive understanding of the entire image. Therefore, this paper compares and analyzes the performance of the neural network models VGG16 [15], InceptionV3 [16, 17] and ResNet50 [18, 19] on PCB defect detection. In order to further improve the recognition accuracy of the model, an improved network model structure is proposed based on the ResNet50 network structure. In the ResNet50 model, a CNN module Res2Net is introduced, which replaces the residual block of the original convolutional layer with a more hierarchical residual connection structure. ReLU is used as the activation function behind each BottleNeck to improve the non-linear expansion capability of the network's multi-layers.

2 PCB Defect Types and Dataset Construction

2.1 PCB Defect Types

PCB defect images are mainly obtained by the automated visual inspection (AVI) system in a PCB manufacturing company. The common PCB defects are usually divided into nine categories, namely: gold cavity, fracture, chromatic aberration, skip plating, delamination, appearance burr, scratch, residue and foreign matter. The specific PCB defect images are shown in Fig. 1. For a huge image data set, the image number of each PCB defect type is uneven. Some defect types have very few images, but some defect types have a large number of images. Among them, residue (abbreviated as RE-CU) and foreign matter (abbreviated as FB-CU), are the most common defects and the number of appearances is particularly high [20]. Nevertheless, the number of other types of defects is relatively small. Therefore, this paper mainly uses these two types of defective images (RE-CU and FB-CU), and the images without defect as datasets for training, validation and testing.

2.2 PCB Dataset Construction

The aim of this study is to identify whether there are defects in the PCB. The collected image samples are divided into two types: defective (NG) and non-defective (OK). NG defective pictures mainly include the residue (RE-CU) and foreign matter (FB-CU), which are the two most numerous defect types, as shown in the Fig. 2.

The PCB image size is unified to 224×224 size in the image pre-processing stage. The image transformation is utilized to enhance the diversity of data and improve the robustness of the network. The common data augmentation methods include left–right flip, up-down flip, rotation, scaling, and clipping. By using data augmentation technology, the number of images, which can be used for training, verification and testing, is increased several times to improve the testing accuracy of the model and to enhance the diversity of data and improve the robustness of the network.

In order to expand the number of samples in the data set, the original training image data set is augmented using the data augmentation method [20, 21]. Both the training and test sets before and after data augmentation are divided into two categories: defective (NG) and non-defective (OK). The training set data is enhanced from the original 5200 NG images (2600 and 2600 for residue, foreign matter respectively) and 5200 OK images to 10,400 NG images (5200 and 5200 for residue, foreign matter respectively) and 10,400 OK images. In addition, the test set remained unchanged, with a total of 5200 images (1300, 1300 and 2600 for residue, foreign matter and defect free types, respectively).

3 Classification Experiment and Result Analysis Based on Three Convolutional Neural Network Models

3.1 Model Training Parameters

In the experiments, the hardware devices such as Intel Core i7-9750H cpu @ 2.60 GHz processor, 16G running memory, and graphics card model NVIDIA GeFoce GTX 1660 Ti are used. The operating system is Windows 10, the

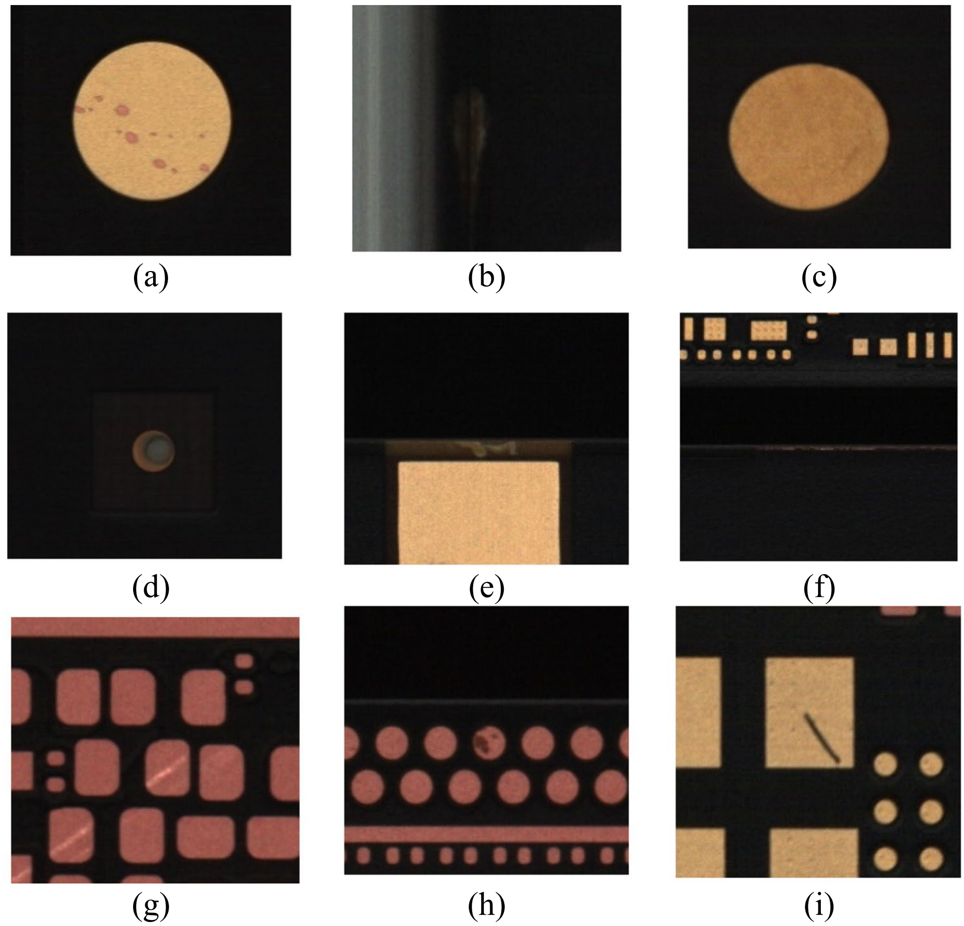

Fig. 1 PCB defect image categories: (**a**) Gold cavity. (**b**) Fracture. (**c**) Chromatic aberration. (**d**) Skip plating. (**e**) Delamination. (**f**) Appearance burr. (**g**) Scratch. (**h**) Residue. (**i**) Foreign matter

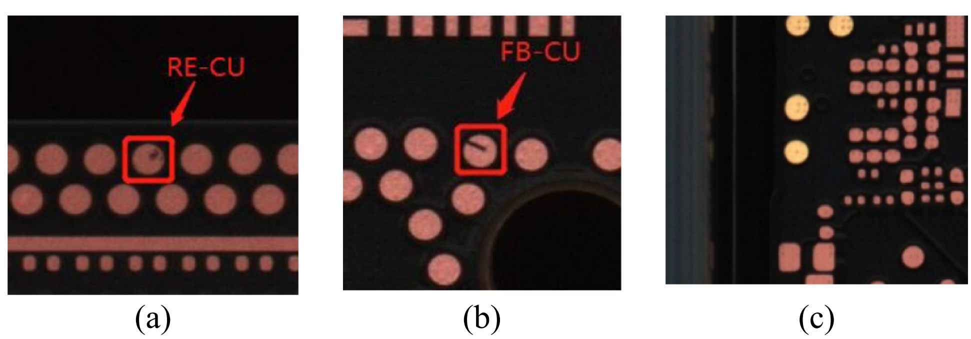

Fig. 2 Image samples: (**a**) Residue (RE-CU). (**b**) Foreign matter (FB-CU). (**c**) Non-defective (OK)

programming language is Python 3.6, and the deep learning framework is Pytorch.

The three convolutional neural network models, VGG16, InceptionV3, and ResNet50, are used for training respectively. The parameters of different models are optimized and adjusted according to the experimental results. The final selected optimal training parameters are as follow:

1) Iteration times:150;
2) Batch_size:32;
3) Basic learning rate:0.01;
4) Loss function: Cross entropy;
5) Learning rate adjustment strategy: Reduce LR ON Plateau;
6) Attenuation constant:0.1.

In addition, the cross-entropy loss function is used in the training process, and the network parameters are updated using the strategy of SGD. Then in order to evaluate the classification performance of each model, the data such as loss function and verification accuracy during training are visualized. The standards of Accuracy, Precision, Specificity, Sensitivity (Recall) and F1 are utilized to measure the classification of the model, which are similar to the reference [20, 22]. The indicators are calculated based on the confusion matrix in machine learning. TP (True Positive) is the number of positive cases correctly predicted. TN (True Negative) is the number of negative cases correctly predicted. FP (False Positive) is the number of negative cases wrongly predicted as positive. FN (False Negative) is the number of positive cases wrongly predicted as negative.

3.2 Experimental Results and Analysis

In purpose of comparing the classification effects of the three models, the training loss values and validation accuracy of the three models are plotted in the same figure respectively.

The training loss and accuracy variation graphs for the three models are shown in Fig. 3. As can be seen from Fig. 3a, the ResNet50 model converges slightly faster and converges better than the other two models. Meanwhile, the convergent loss values of the VGG16 and InceptionV3 models are higher than that of the ResNet50 model, indicating that the ResNet50 model fits better. The graphs of the verification accuracy changes for the three models are shown in

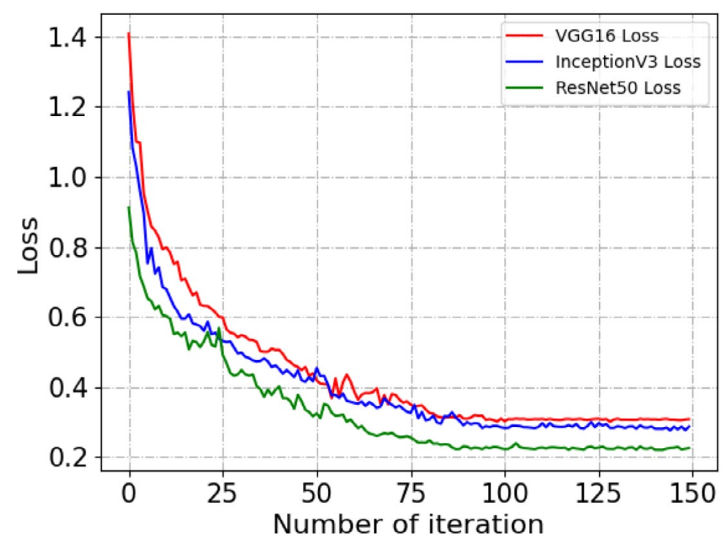

(a)

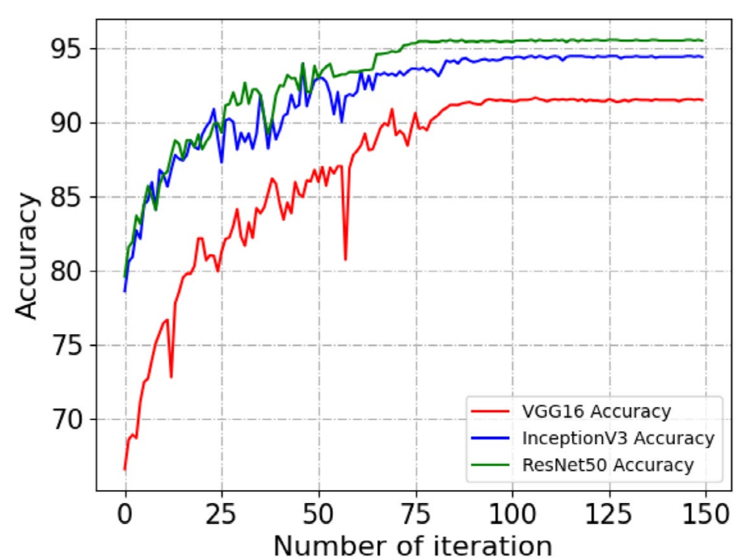

(b)

Fig. 3 Curve graphs of three models: (**a**) Training loss curve. (**b**) Training accuracy curve

Fig. 3b. It can be seen that the overall verification accuracy of the ResNet50 model is higher than those of the VGG16 and InceptionV3 models during the training process. It can reach 0.9549, which verifies that the stability of the accuracy curve is better.

The performances of the three different models under the testing set are obtained. Through the analysis of the results, it can be found that the accuracy of the ResNet50 network is 95.7%, the accuracy of the InceptionV3 network reached 94.6% and the VGG16 network has the lowest accuracy of 91.3%.

The three models were trained with optimal parameters and tested on the same test set. The obtained accuracy, precision, sensitivity, specificity and F1 value are shown in Table 1. The performance indicators of VGG16 model respectively has reached 91.3%, 95.8%, 86.3%, 96.2% and 90.8%; The performance indicators of InceptionV3 model respectively has reached 94.6%, 95.9%, 93.2%, 96.0% and 94.5%; The performance indicators of ResNet50 model respectively has reached 95.7%, 97.3%, 93.9%, 97.4% and 95.6%.

The depth of the InceptionV3 network and the ResNet network is deeper than that of the VGG16 network. It can be seen that the deeper the network, the better the effect of extracting features. The ResNet50 model can guarantee a high recall rate (sensitivity) under the premise of high accuracy and precision. This shows that the number of NG images recognized correctly is relatively higher than that of other models and more NG images are recognized. In addition, the F1 value of the ResNet50 network is also the highest, the performance and the classification effect of the trained model are better. In summary, from the training loss value, accuracy and test indicators of the three models, the ResNet50 model has the best results on various indicators compared to the VGG16 and InceptionV3 models. It shows a better feature extraction effect in the PCB image set. The model performance is superior and more suitable for PCB image classification and recognition tasks.

3.3 Impact of Data Augmentation

In order to compare the effect of model classification before and after data augmentation, the model training loss value and the verification accuracy of ResNet50 before and after data augmentation are respectively plotted on the same coordinate axis, as shown in Fig. 4. It can be seen from Fig. 4a that the model after data augmentation has a faster convergence speed and a better convergence effect. At the same time, the loss value of convergence is smaller. This shows that the model after data augmentation fits better. Figure 4b shows the change of verification accuracy before and after data augmentation. The overall model verification accuracy after data augmentation is higher than that before data augmentation and it can reach up to 0.9750 in Fig. 4b.

Table 1 Optimal training parameters for each network model

Model	Accuracy	Precision	Sensitivity	Specificity	F1 value
VGG16	91.3%	95.8%	86.3%	96.2%	90.8%
InceptionV3	94.6%	95.9%	93.2%	96.0%	94.5%
ResNet50	95.7%	97.3%	93.9%	97.4%	95.6%

The accuracy, precision, sensitivity, specificity and F1 value of the ResNet50 before and after data augmentation are shown in Table 2. Before data augmentation, performance indicators of ResNet50 model respectively have reached 95.7%, 97.3%, 93.9%, 97.4% and 95.6%. After data augmentation, performance indicators of ResNet50 model respectively have reached 97.8%, 99.8%, 95.8%, 99.8% and 97.7%.

It can be seen that the model after data augmentation achieves the best performance with 2.1% higher in accuracy, 2.5% higher in precision, 1.9% higher in sensitivity, 2.4% higher in specificity, and 2.1% higher in F1 value than that of the model before data augmentation. In summary, the various indicators of the model can be improved through data augmentation. The PCB classification performance of the model has been improved.

4 Improved Network Architecture

4.1 ResNet50 Network Structure Improvement

Compared with the VGG16 and InceptionV3 networks, the number of ResNet network layers is not very deep, the network parameters are relatively small, and the convergence speed is faster. However, according to the above experiments, it is found that the sensitivity of the ResNet50 model after data augmentation is 95.8%. According to the experimental results, it is found that the size of many defects in unrecognized NG images is smaller than the general defect size. The feature is easy to be ignored when the network is performing feature extraction. After statistics, it is found that 112 images in the 5200 PCB testing set have small defects. The above-mentioned ResNet50 model only recognizes 38 images correctly, and the recognition accuracy of small defect images is less than 34%. It can be seen that while improving the accuracy of the overall defect image recognition, it is also necessary to improve the recognition ability of some small defects.

During the training process, some feature information in the defective images may be lost as the number of network

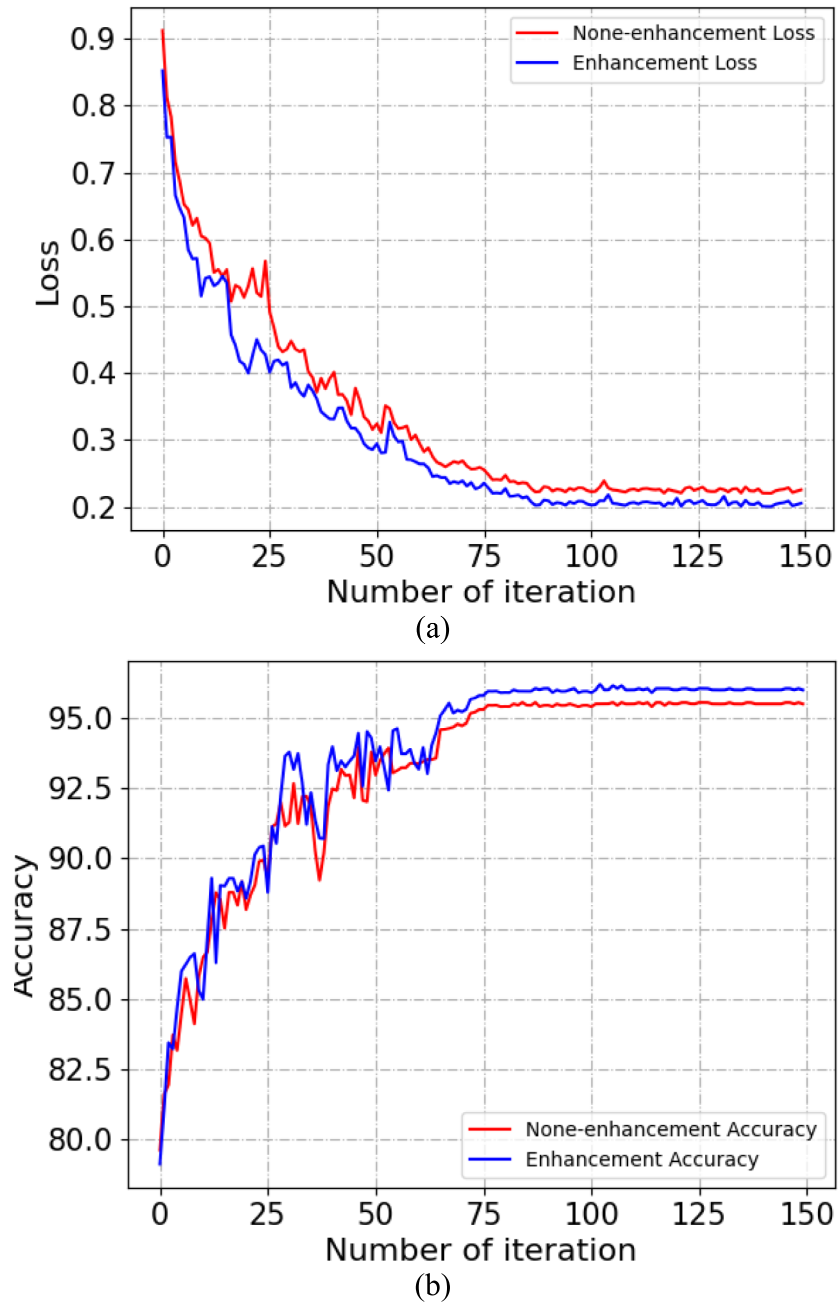

Fig. 4 Curve graphs of the model before and after data augmentation: (**a**) Training loss curves. (**b**) Training accuracy curves

Table 2 Performance indicators of ResNet50 before and after data augmentation

	Accuracy	Precision	Sensitivity	Specificity	F1 value
Before data augmentation	95.7%	97.3%	93.9%	97.4%	95.6%
After data augmentation	97.8%	99.8%	95.8%	99.8%	97.7%

layers increases step by step. In order to extract feature information more efficiently and represent multi-scale features at a finer-grained level, a new CNN module called Res2Net is introduced [23–25]. It will combine the original ResNet50 model to improve the ability to recognize defective images.

Previous networks use features of different resolutions to improve multi-scale capabilities. The Res2Net module is different from the previous network structure. It constructs a hierarchical similar residual connection within a single residual block, which can represent multi-scale features at a finer-grained level and increase the receptive field of each

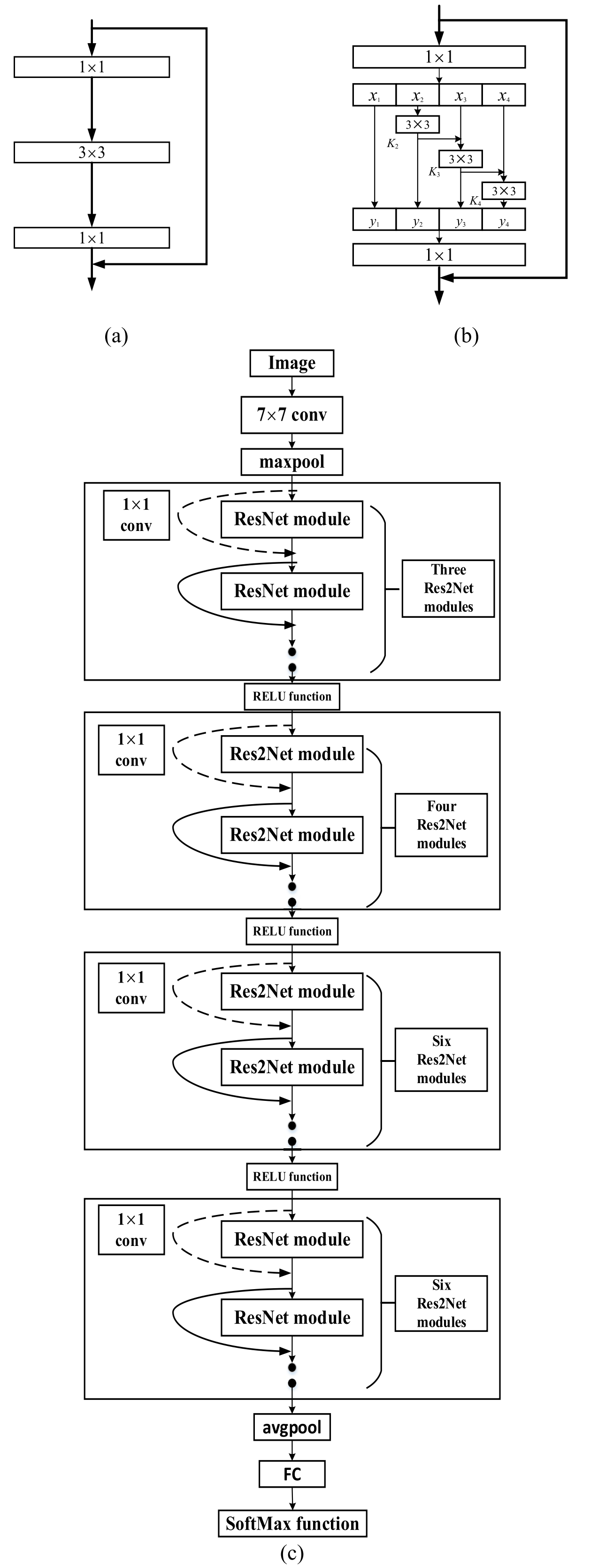

Fig. 5 Comparison of blocks in ResNet model and Res2Net module: (**a**) Resnet Bottleneck block. (**b**) Res2net module. (**c**) Modified-ResNet50 model structure after improvement

network. The stronger the ability of the model to extract the features is, the stronger the ability of the classification is. Figure 5a is a block in the ResNet network, and Fig. 5b is a single residual unit of Res2Net. It can be seen that the latter inserts more hierarchical residual connection structure in the residual block.

The module replaces the 3×3 convolution kernel of n channels with a smaller set of filter banks, and connects different filter banks in a hierarchical-like residual manner. As shown in Fig. 5b, after the first 1×1 convolution, the input is divided into s subsets. It is defined as:

$$x_i, i \in \{1,2,3 \cdots s\} \tag{1}$$

Each feature has the same size, but the channel is 1/s of the input feature. Except for x_1, other sub-features have corresponding 3×3 convolution kernels, which are defined as $k_i()$, and their output is y_i. In order to reduce the number of model parameters when increasing the number of subsets s, the 3×3 convolution kernel of x_1 is omitted. Therefore, the output y_i is written as:

$$y_i = \begin{cases} x_i & i = 1 \\ k_i(x_i) & i = 2 \\ k_i(x_i + y_{i-1}) & 2 < i \le s \end{cases} \tag{2}$$

Each 3×3 convolution operation can potentially accept all the feature information by the output of the previous layer, and each output can increase the receptive field. As a result, each Res2Net can obtain feature combinations of different number and different receptive field size. Therefore, integrating the Res2Net module into the above ResNet50 model can improve the extraction and recognition capabilities of defect features. The improved ResNet50 network structure is shown in Fig. 5c.

The specific modification is as follows: based on the ResNet50 model structure, the Res2Net module is integrated into the ResNet50 structure. The ResNet50 model has a total of 50 layers, consisting of four large blocks, each of which has 3, 4, 6, and 3 small blocks. And each small block has three convolutional layers. Based on this foundation, the multiple small blocks in the second and third large BottleNeck are replaced with Res2Net modules. Then the other two large BottleNecks are connected in the original order. In addition, ReLU is used as the activation function behind each large BottleNeck to improve the non-linear scalability of the network multilayers.

4.2 Experiments and Result Analysis

In the experiment, the improved ResNet50 model is used as the deep convolutional neural network model. The image samples after data augmentation are used as

Fig. 6 Curves graphs of the improved ResNet50 model: (**a**) Training-validation loss curves. (**b**) Training-validation accuracy curves

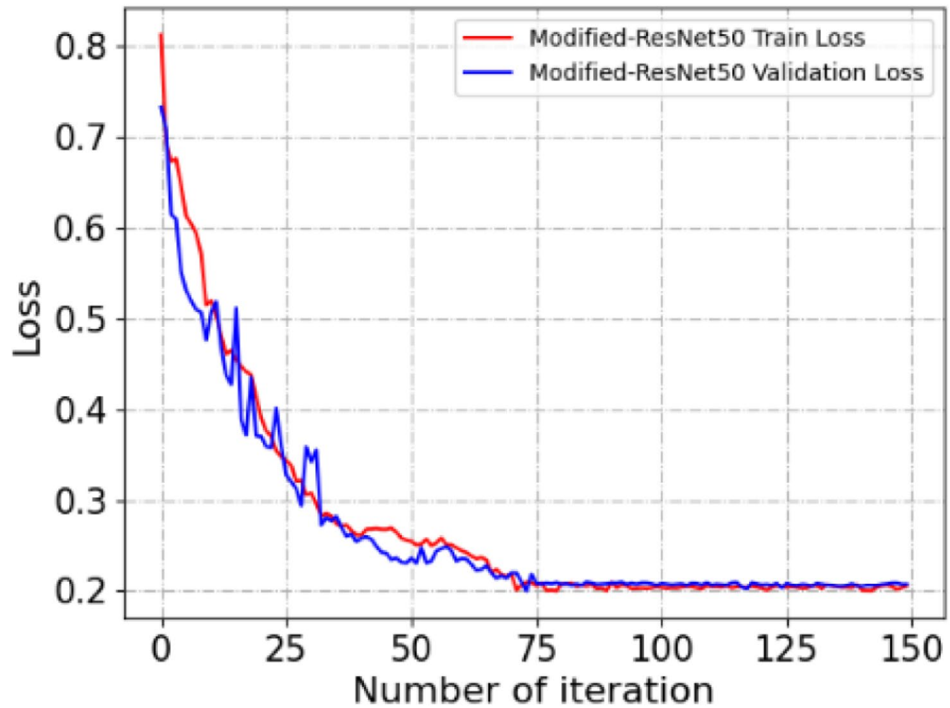

(a)

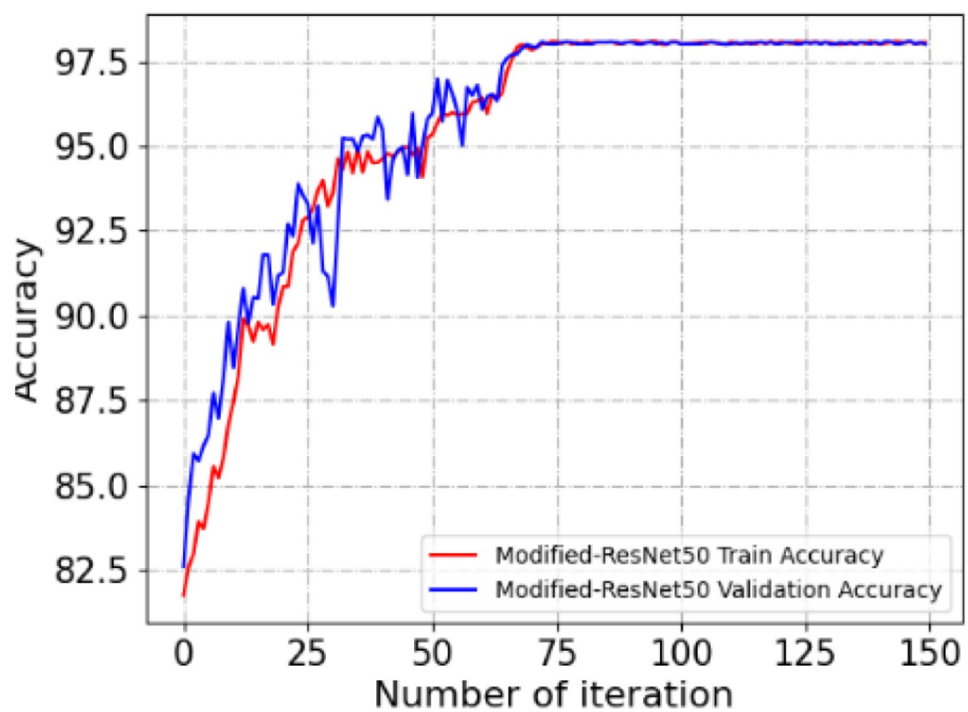

(b)

experimental data. The training loss value and the verification loss value change with the number of training iterations are shown in Fig. 6a. As the number of iterations increases, the training loss value and the verification loss value generally show a decreasing trend. Finally, they stabilize around 60 iterations, and the final loss values tend to 0.20, indicating that the network is close to convergence at this time. The change curves of training accuracy and

Table 3 Performance indicators of the original ResNet50 model and the improved ResNet50 model

Model	Accuracy	Precision	Sensitivity	Specificity	F1 value
Original ResNet50	97.8%	99.8%	95.8%	99.8%	97.7%
Improved ResNet50	98.3%	97.9%	98.7%	97.9%	98.3%

Table 4 Small defect image recognition results of the original ResNet50 model and the improved ResNet50 model

Model	Total number of small defects	Number of correct recognitions	Accuracy
Original ResNet50	112	38	33.9%
Improved ResNet50	112	99	88.4%

verification accuracy are shown in Fig. 6b. It is obvious that the training accuracy and verification accuracy generally increase with the increase in the number of iterations, and finally stabilize at 0.9781.

The accuracy, precision, sensitivity, specificity and F1 value of the ResNet50 before and after optimized are shown in Table 3. Before optimized, performance indicators of model respectively have reached 97.8%, 99.8%, 95.8%, 99.8% and 97.7%. After optimized, performance indicators of model respectively have reached 98.3%, 97.9%, 98.7%, 97.9% and 98.3%.

The improved Modified-ResNet50 model has a 0.5% higher recognition accuracy and a 1.9% lower precision than the ResNet50 model on the same test set. The sensitivity, specificity and F1 value of the improved ResNet50 model are 2.9% higher, 1.9% lower and 0.6% higher than that of the ResNet50 model, respectively.

Table 4 shows the improved ResNet50 model and the original ResNet50 model's recognition of small defect images in the test set. It can be found from Table 4 that the improved ResNet50 model has improved the accuracy of recognizing small defects from 33.9% to 88.4%. The improved ResNet50 model has greatly improved the ability to recognize small defects. In summary, the improved model has improved PCB defect recognition ability. Although the precision and specificity have been reduced, the overall model has a better classification effect in PCB defect classification tasks.

In order to test the PCB image recognition ability of the improved model, the sensitivity and the specificity of the improved ResNet50 model under different thresholds were tested. The number of images in the testing set remains the same. It is determined whether the image is recognized as NG by comparing the image probability with the threshold. Figure 7 shows the sensitivity and specificity curves of the improved ResNet50 model under different thresholds. It can be seen from Fig. 7 that the sensitivity decreases and the specificity increases as the threshold increases. It shows

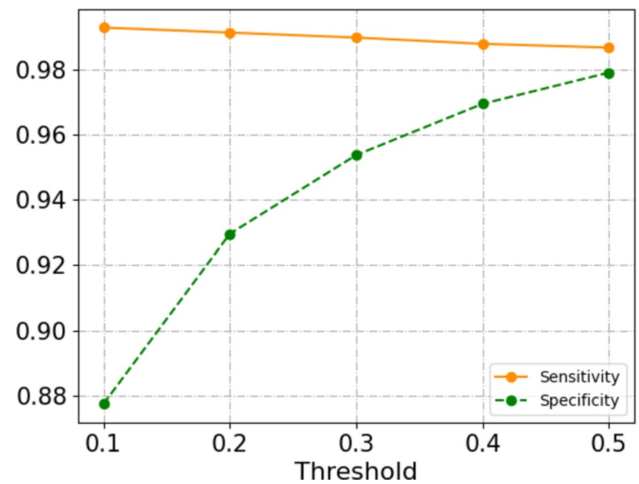

Fig. 7 Sensitivity and specificity of the improved ResNet50 model under different thresholds

that the improved ResNet50 model has a higher recognition accuracy for NG PCB images at a lower threshold. The sensitivity can reach 99.3% under the 0.1 threshold, which can basically meet the PCB defect detection requirements in industrial production.

5 Conclusion

This paper introduces the convolutional neural network into the classification and recognition of PCB defect images. The three convolutional neural network classification models of VGG16, InceptionV3 and ResNet50 are studied. Based on the constructed PCB image data set, these three network models are trained, and the performance of the trained model is tested using the test set. The results show that the ResNet50 model has a better PCB defect image classification effect than the VGG16 and InceptionV3 models. The two data sets before and after data augmentation are compared through experiments. The results show that even without increasing the number of PCB image samples, the method of data augmentation can improve the classification and recognition accuracy of the ResNet50 model. Based on the analysis of the ResNet50 network structure, an improved network model structure is developed. In the ResNet50 model, a new type of CNN module Res2Net is introduced, which replaces the original residual block of the convolutional layer with a more layered residual connection structure. The ReLU is used as the activation function behind each BottleNeck to improve the non-linear expansion capability of the network. The comparative experiments show that the improved ResNet50 model has a better classification effect in the PCB defect classification task, and the sensitivity of the model reached 99.3% under the threshold of 0.1.

Acknowledgements This research was supported by the National Natural Science Foundation of China (No. 52175102).

Data Availability The data that support the findings of this study are available upon reasonable request from the authors.

Declarations

Conflicts of Interests/Competing Interests The authors declare that they have no known competing financial interests or personal relationships that could have appeared to influence the work reported in this paper.

References

1. Adibhatla VA, Chih HC, Hsu CC, Cheng J, Abbod MF, Shieh JS (2020) Defect detection in printed circuit boards using you-only-look-once convolutional neural networks. Electron 9(9):1547
2. Kumar P, Shreekanth T, Prajwal MR (2020) Automated quality inspection of PCB assembly using image processing. Int J Image Graphics Signal Process 12(3):13–19
3. Chen IC, Hwang RC, Huang HC (2023) Pcb defect detection based on deep learning algorithm. Processes 11(3):775
4. Ran G, Lei X, Li D, Guo Z (2020) Research on PCB defect detection using deep convolutional neural network. In: 5th International Conference on Mechanical, Control and Computer Engineering (ICMCCE), pp 1310–1314
5. Parakontan T, Sawangsri W (2019) Development of the machine vision system for automated inspection of printed circuit board assemblies. In: 3rd International Conference on Robotics and Automation Sciences (ICRAS), pp 244–248
6. Kuo CFJ, Fang TY, Lee CL, Wu HC (2019) Automated optical inspection system for surface mount device light emitting diodes. J Intell Manuf 30(2):641–655
7. Wu F, Zhang X, Kuan Y, He Z (2008) An AOI algorithm for PCB based on feature extraction. In: 7th World Congress on Intelligent Control and Automation, pp 240–247
8. Hassanin AAI, Abd El-Samie FE, Banby GME (2019) A real-time approach for automatic defect detection from PCBs based on SURF features and morphological operations. Multimedia Tools Appl 78(24):34437–34457
9. Liu Z, Qu B (2021) Machine vision based online detection of PCB defect. Microprocess Microsyst 82:103807
10. Wu X, Ge Y, Zhang Q, Zhang D (2021) PCB defect detection using deep learning methods. In: IEEE 24th International Conference on Computer Supported Cooperative Work in Design (CSCWD), pp 873–876
11. Huang W, Wei P, Zhang M, Liu H (2020) HRIPCB: a challenging dataset for PCB defects detection and classification. J Eng 13:303–309
12. Kim YG, Lim DU, Ryu JH, Park TH (2018) SMD defect classification by convolution neural network and PCB image transform. In: IEEE 3rd International Conference on Computing, Communication and Security (ICCCS), pp 180–183
13. Deng YS, Luo AC, Dai MJ (2018) Building an automatic defect verification system using deep neural network for PCB defect classification. In: 4th International Conference on Frontiers of Signal Processing (ICFSP), pp 145–149
14. Cheong LK, Suandi SA, Rahman S (2019) Defects and components recognition in printed circuit boards using convolutional neural network. In: 10th International Conference on Robotics, Vision, Signal Processing and Power Applications: Enabling Research and Innovation towards Sustainability, pp 75–81
15. Omiotek Z, Kotyra A (2021) Flame image processing and classification using a pre-trained VGG16 model in combustion diagnosis. Sens 21(2):500
16. Khan RU, Zhang X, Kumar R (2019) Analysis of ResNet and GoogleNet models for malware detection. J Comput Virol Hacking Tech 15(1):29–37
17. Szegedy C, Liu W, Jia Y, Sermanet P, Reed S, Anguelov D, Erhan D, Vanhoucke V, Rabinovich A (2015) Going deeper with convolutions. In: IEEE Conference on Computer Vision and Pattern Recognition (CVPR), pp 1–9
18. He K, Zhang X, Ren S, Sun J (2016) Deep residual learning for image recognition. In: IEEE Conference on Computer Vision and Pattern Recognition (CVPR), pp 770–778
19. Theckedath D, Sedamkar R (2020) Detecting affect states using VGG16, ResNet50 and SE-ResNet50 networks. SN Comput Sci 1(2):1–7
20. Zhang J, Chang Z, Xu H, Qu D, Shi X (2024) Printed circuit board defect image recognition based on the multimodel fusion algorithm. J Electron Packag 146(2):021009
21. Wang C, Huang G, Huang Z, He W (2023) Conditional TransGAN-based data augmentation for PCB electronic component inspection. Comput Intell Neurosci 2023(1):2024237
22. Alelaumi S, Wang H, Lu H, Yoon SW (2020) A predictive abnormality detection model using ensemble learning in stencil printing process. IEEE Trans Compon Packag Manuf Technol 10(9):1560–1568
23. Gao SH, Cheng MM, Zhao K et al (2019) Res2net: a new multi-scale backbone architecture. IEEE Trans Pattern Anal Mach Intell 43(2):652–662
24. Zhou W, Chen Y, Liu C, Yu L (2020) GFNet: Gate fusion network with Res2Net for detecting salient objects in RGB-D images. IEEE Signal Process Lett 27:800–804
25. Yang C, Guo Z, Liu Y (2020) Fast and precise energy consumption prediction based on fully convolutional attention Res2Net. In: ACM Turing Celebration Conference, pp 185–189

Jiantao Zhang is a professor in the School of Mechatronic Engineering and Automation of Shanghai University. He received the B.S. and M.S. degrees from Hefei University of Technology, China, in 2002, 2005 and the Ph.D. degree from Nanjing University of Aeronautics and Astronautics, China, in 2009. His research interests include PCB inspection technology based on artificial intelligence, advanced robotics technology, micro energy harvesting and intelligent sensing.

Xinyu Shi received the B.S. degree in mechanical engineering and automation from Central South University of Forestry and Technology, Changsha, China, in 2022. He is currently pursuing his M.S. degree in mechanical manufacturing and automation at Shanghai University. His research interests include PCB defect detection and deep learning.

Dong Qu received the B.S. degree in mechanical engineering and automation from Yangzhou University, Jiangsu, China, in 2018. He received the M.S. degree in mechanical manufacturing and automation at Shanghai University, Shanghai, China, in 2021. His research interests include convolutional neural networks and PCB defect detection technology.

Haida Xu received the B.S. degree in mechanical engineering and automation from Hangzhou City University, Zhejiang, China, in 2020. He received the M.S. degree in mechanical manufacturing and automation at Shanghai University, Shanghai, China, in 2023. His research interests include PCB defect detection and artificial intelligence.

Zhengfang Chang received the B.S. degree in mechanical engineering and automation from Zhejiang Normal University, Zhejiang, China, in 2021. He received the M.S. degree in mechanical manufacturing and automation at Shanghai University, Shanghai, China, in 2024. His research interests include convolutional neural networks and their applications in PCB defect detection.